











## RESEARCH ARTICLE

View Article Online  
View Journal | View IssueCite this: *Org. Chem. Front.*, 2023, **10**, 2913

# Ratiometric sensing of $\beta$ -galactosidase based on excited-state intramolecular proton transfer (ESIPT) and solid-state luminescence enhancement†

 He Tian, Jr., <sup>a</sup> Wei Lin, <sup>a</sup> Xi-Le Hu, <sup>a</sup> Jing-Bo Wang, <sup>a</sup> Min-Yu Zhang, <sup>a</sup>  
 Yi Zang, <sup>b,f,g</sup> Xin-Yan Wu, <sup>a</sup> Jia Li, <sup>\*b,f</sup> Tony D. James <sup>\*d,e</sup> and  
 Xiao-Peng He <sup>\*a,c</sup>

Glycosidases play important roles in modulating the structural and functional integrity of glycoproteins and glycolipids, and thus are promising biomarkers for disease diagnosis. While current approaches for glycosidase detection mainly rely on an enhancement of the UV-vis absorbance or fluorescence emission of glycosyl indicators, here we develop a ratiometric fluorescent probe for the sensitive and selective detection of glycosidase activity based on the combined mechanisms of excited-state intramolecular proton transfer (ESIPT) and solid-state luminescence enhancement (SSLE). The probe behaves like a typical SSLE when glycosylated, and exhibits a ~140 nm red-shift in fluorescence owing to activation of ESIPT after deglycosylation. Such a large Stokes shift may facilitate the unbiased analysis of glycosidase activities when used in diagnostic and drug-screening assays.

Received 23rd April 2023,  
Accepted 9th May 2023

DOI: 10.1039/d3qo00605k

rsc.li/frontiers-organic

Glycosylation and deglycosylation reactions of biomacromolecules including proteins, peptides and lipids are implicated in a myriad of biological and pathological processes.<sup>1–3</sup> Deglycosylation is the removal of a glycosyl residue from a glycoconjugate as mediated by glycosidases, which are conserved in almost all eukaryotes. In human cells, they mainly distribute in the endoplasmic reticulum (ER), Golgi apparatus and

lysosomes.<sup>4,5</sup> Glycosidases localized in the ER and Golgi apparatus are responsible for tailoring the *N*-glycans on proteins after translation, and lysosomal glycosidases are known to hydrolyze the glycosyl residues on glycoconjugates endocytosed by cells.

However, the abnormal expression of glycosidases is associated with human diseases. For example, during cell senescence,  $\beta$ -galactosidase ( $\beta$ -Gal) and  $\alpha$ -fucosidase are overly expressed,<sup>6,7</sup> and the abnormally high expression of  $\beta$ -Gal is closely related to the tumorigenesis and metastasis of ovarian cancer.<sup>8</sup> In addition, a recent proteomics study suggests that the expression level of cytoplasmic  $\beta$ -glucocerebrosidase in liver cancer tissues is significantly lower than that in para-carcinoma tissues.<sup>9</sup> As a consequence, the effective detection of glycosidase activities is important for glycobiological studies and disease diagnosis.

The current approaches for analysis of glycosidase activity mainly rely on colorimetric assays, which use glycosylated indicators such as 4-nitrophenol as the colorimetric substrate. However, assays that are dependent on color changes are easily compromised by the intrinsic color of the sample itself and are generally of low sensitivity. To overcome these issues, activatable fluorescent probes that exhibit a “turn-on” fluorescence upon enzymatic hydrolysis have been developed.<sup>10–17</sup> Based on a variety of fluorescent dyes, molecular probes capable of sensing glycosidases in cells and *in vivo* with emission wavelengths that range from the visible to the near-infrared region, have been synthesized in recent years.<sup>18–27</sup>

<sup>a</sup>Key Laboratory for Advanced Materials and Joint International Research Laboratory of Precision Chemistry and Molecular Engineering, Feringa Nobel Prize Scientist Joint Research Center, School of Chemistry and Molecular Engineering, East China University of Science and Technology, 130 Meilong Rd, Shanghai 200237, China. E-mail: xphe@ecust.edu.cn

<sup>b</sup>National Center for Drug Screening, State Key Laboratory of Drug Research, Shanghai Institute of Materia Medica, Chinese Academy of Sciences, Shanghai 201203, China. E-mail: jli@simm.ac.cn

<sup>c</sup>National Center for Liver Cancer, The International Cooperation Laboratory on Signal Transduction, Eastern Hepatobiliary Surgery Hospital, Shanghai 200438, China

<sup>d</sup>Department of Chemistry, University of Bath, Bath, BA2 7AY, UK. E-mail: t.d.james@bath.ac.uk

<sup>e</sup>School of Chemistry and Chemical Engineering, Henan Normal University, Xinxiang 453007, China

<sup>f</sup>School of Pharmaceutical Science and Technology, Hangzhou Institute for Advanced Study, University of Chinese Academy of Sciences, Hangzhou 310024, China

<sup>g</sup>Lingang Laboratory, Shanghai 201203, China

† Electronic supplementary information (ESI) available: Additional figures, experimental section and original spectral copies of new compounds. See DOI: <https://doi.org/10.1039/d3qo00605k>



Here, we report the construction of a ratiometric fluorescent probe that exhibits a large Stokes shift of the fluorescence emission wavelength upon hydrolysis by glycosidases based on the combination of excited-state intramolecular proton transfer (ESIPT) and solid-state luminescence enhancement (SSLE).<sup>28–30</sup> The probe is a typical SSLE system when glycosylated, and after deglycosylation, the ESIPT process is activated, thereby achieving a ~140 nm red-shift in fluorescence emission.

To construct the ratiometric glycosidase probe, we first synthesized a fluorescent reporter with dual photophysical mechanisms. In the *ortho* position relative to the phenol group of tetraphenylethylene (TPE), benzothiazole (BT) was introduced. The resulting conjugate (**TPE-BT**) formed by the cycloaddition of 2-hydroxy-5-(1,2,2-triphenylethenyl)-benzaldehyde and 2-aminothiophenol exhibits ESIPT due to the intramolecular hydrogen bonding interaction between the nitrogen atom and the phenolic proton.<sup>31,32</sup> Then, galactose was introduced to the phenolic site to inhibit ESIPT by removing the hydrogen-bond donor. A benzyl group was used to connect the **TPE-BT** and galactose (producing the **Gal-TPE-BT** probe) in order to enhance the sensitivity for glycosidases.<sup>33</sup> After deglycosylation, the benzyl moiety undergoes a “self-immolation” process resulting cleavage (Fig. 1), thereby recovering the ESIPT nature of **TPE-BT**. The synthetic details for the probe are shown in Scheme S1.†

With the probe in hand, we evaluated its photophysical properties in the absence and presence of  $\beta$ -Gal.  $\beta$ -Gal isolated from *Escherichia coli* was used as a model enzyme for the analysis. We first determined that **Gal-TPE-BT** exhibited typical SSLE properties. The fluorescence of the probe (excited at 360 nm) was negligible in dimethyl sulfoxide (DMSO) as the good solvent, whereas a gradual increase in the H<sub>2</sub>O fraction of the solvent system led to a gradual fluorescence enhancement at  $\lambda_{\text{max}} = 470$  nm, which is characteristic of TPE (Fig. 2a and b). The fluorescence of the probe dropped slightly in pure water, which is common for TPE-based fluorogens.<sup>34</sup> This

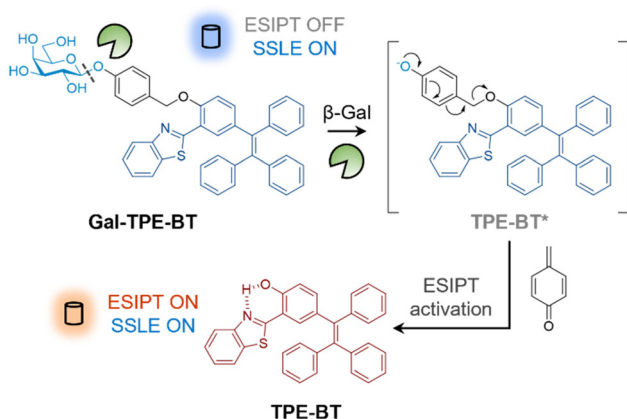


**Fig. 1** Schematic illustration of the ratiometric detection of  $\beta$ -galactosidase based on excited-state intramolecular proton transfer (ESIPT) and solid-state luminescence enhancement (SSLE).

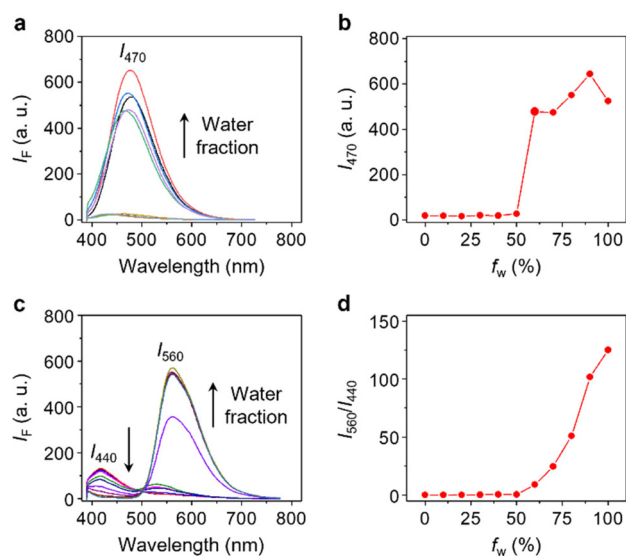


**Fig. 2** Fluorescence emission spectra of (a) **Gal-TPE-BT** (10  $\mu$ M) and (c) **TPE-BT** (10  $\mu$ M) in DMSO with increasing water fractions. (b) Plotting the maximum fluorescence emission intensity of **Gal-TPE-BT** at 470 nm in a mixed solvent of H<sub>2</sub>O/DMSO as a function of water fraction ( $f_w$ ). (d) Plotting the ratios of the maximum fluorescence emission intensity of **TPE-BT** at 560 nm and 440 nm in a mixed solvent of H<sub>2</sub>O/DMSO as a function of water fraction ( $f_w$ ). The excitation wavelength used for **Gal-TPE-BT** and **TPE-BT** is 360 nm.

suggests the successful suppression of the ESIPT process in **Gal-TPE-BT** through the masking of the phenolic proton.

In the presence of  $\beta$ -Gal, the fluorescence emission spectra of **Gal-TPE-BT** in mixed H<sub>2</sub>O/DMSO solvents changed substantially (Fig. 2c). We observed a new red-shifted emission band with  $\lambda_{\text{max}}$  at 560 nm that was sharply enhanced as the water fraction increased, and the original emission band with  $\lambda_{\text{max}}$  at 440 nm gradually decreased. The newly emerged emission band is assignable to the keto-state emission of **TPE-BT**,<sup>31</sup> suggesting the recovery of the ESIPT mechanism of the probe.<sup>35,36</sup> More interestingly, the gradually enhanced fluorescence at  $\lambda_{\text{max}} = 560$  nm with increasing water fraction suggests the maintenance of the SSLE mechanism in **TPE-BT**, which favours sensing applications in an aqueous phase.

To confirm the enzymatic hydrolysis, mass spectroscopic (MS) analysis generated a MS peak assignable to **TPE-BT** detected after treatment of **Gal-TPE-BT** with  $\beta$ -Gal (Fig. S1†), corroborating that the galactosyl substrate can be deglycosylated by the enzyme. We also determined that the ratiometric fluorescence changes ( $I_{560}/I_{440}$ ) of the probe were dependent on the concentration of  $\beta$ -Gal (Fig. 3a), and a good linearity from 1–6 U mL<sup>-1</sup> was determined (Fig. 3b). The limit of detection of the probe for  $\beta$ -Gal was determined to be 0.03 U mL<sup>-1</sup> ( $3\sigma/k$ , where  $\sigma$  is the standard deviation of ten blank samples, and  $k$  is the linear slope of the ratiometric changes of the probe as a function of  $\beta$ -Gal concentration). In addition, a kinetic study indicated a 13.5-fold increase in the  $I_{560}/I_{440}$  ratio after the reaction between the probe and the enzyme for 300 min (Fig. S2a and b†), and the  $K_m$  and  $V_{\text{max}}$  were deter-



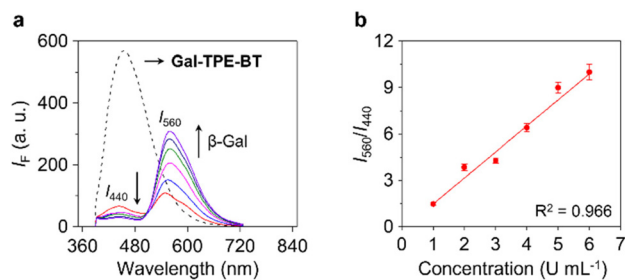


**Fig. 3** (a) Fluorescence emission spectra of Gal-TPE-BT (10  $\mu\text{M}$ ) incubated with increasing concentrations of  $\beta\text{-Gal}$  (0–6  $\text{U mL}^{-1}$ ) for 2 h. (b) Plotting the ratios of the maximum fluorescence emission intensity of Gal-TPE-BT (10  $\mu\text{M}$ ) after treatment with increasing concentrations of  $\beta\text{-Gal}$  (1–6  $\text{U mL}^{-1}$ ) for 2 h at 560 nm and 440 nm as a function of  $\beta\text{-Gal}$  concentration (error bars mean S. D.,  $n = 3$ ). All measurements were performed in a solvent mixture of phosphate buffered saline (PBS) (0.01 M, pH 7.4)/DMSO (7 : 3, v/v) with an excitation of 360 nm.

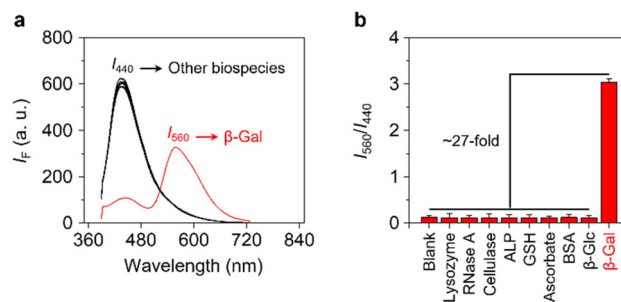


**Fig. 4** (a) Fluorescence emission spectra of Gal-TPE-BT (10  $\mu\text{M}$ ) in the presence of  $\beta\text{-Gal}$  (5  $\text{U mL}^{-1}$ ) and other biospecies including lysozyme (5  $\text{U mL}^{-1}$ ), ribonuclease A (RNase A) (5  $\text{U mL}^{-1}$ ), cellulase (5  $\text{U mL}^{-1}$ ), alkaline phosphatase (ALP) (5  $\text{U mL}^{-1}$ ),  $\gamma$ -glutathione (GSH) (100  $\mu\text{g mL}^{-1}$ ), ascorbate (100  $\mu\text{g mL}^{-1}$ ), bovine serum albumin (BSA) (100  $\mu\text{g mL}^{-1}$ ) and a  $\beta$ -glucosidase ( $\beta\text{-Glc}$ ) (5  $\text{U mL}^{-1}$ ). (b) Plotting the ratios of the maximum fluorescence emission intensity of Gal-TPE-BT (10  $\mu\text{M}$ ) of the different analytes. All measurements were performed in a solvent mixture of phosphate buffered saline (PBS) (0.01 M, pH 7.4)/DMSO (7 : 3, v/v) with an excitation of 360 nm.

mined to be 27  $\mu\text{M}$  and 0.04  $\mu\text{M s}^{-1}$ , respectively, from the Lineweaver–Burk plots (Fig. S2c and d†). We also measured the  $K_m$  and  $V_{\text{max}}$  of a commercial fluorescent  $\beta\text{-Gal}$  probe, 4-methylumbelliferyl- $\beta$ -D-galactoside (4-MU- $\beta\text{-Gal}$ ) (Fig. S3†). The  $\sim$ twofold smaller  $K_m$  of Gal-TPE-BT (27  $\mu\text{M}$ ) than that of 4-MU- $\beta\text{-Gal}$  (48  $\mu\text{M}$ ) suggests a higher affinity of our probe for the enzyme.

Next, we studied the morphological changes of Gal-TPE-BT before and after the enzymatic reaction by high-resolution transmission electron microscopy (HRTEM). In its representative TEM images (Fig. S4†), we observed tube-like structures of Gal-TPE-BT, and after addition of  $\beta\text{-Gal}$ , aggregated particles began to emerge. In addition, DLS (dynamic light scattering) used showed that the hydrodynamic parameter of the probe after reaction with  $\beta\text{-Gal}$  was much larger than that of Gal-TPE-BT without the treatment of  $\beta\text{-Gal}$  (Fig. S5a†). These results corroborate the SSLE property of the probe before and after treatment of the enzyme. The critical micelle concentration (CMC) of the probe was determined to be 5.2  $\mu\text{M}$  (Fig. S5b†), and subsequent DLS and fluorescence analyses by continuously incubating the probe in PBS for 60 h suggest the good colloidal stability of Gal-TPE-BT (Fig. S5c and d†).

Finally, we evaluated the selectivity of Gal-TPE-BT with a range of different biological species (Fig. 4a and b). We determined that the presence of unselective enzymes including lysozyme, ribonuclease A (RNase A), cellulase and alkaline phosphatase (ALP), and biologically relevant species including  $\gamma$ -glutathione (GSH), vitamin C (VC) and bovine serum albumin (BSA) did not cause the fluorescence emission of the probe to change. More importantly, the treatment of Gal-TPE-BT with a  $\beta$ -glucosidase ( $\beta\text{-Glc}$ ) that hydrolyzes glucose, which is the C4-epimer of galactose similarly caused minimal fluctuation in fluorescence of the probe. These results suggest the good selectivity of Gal-TPE-BT for  $\beta\text{-Gal}$  sensing.

To conclude, the incorporation of both ES IPT and SSLE mechanisms into a single molecular probe led us to achieve the ratiometric detection of  $\beta\text{-Gal}$  activity over a range of other

enzymes. The large Stokes shift associated with the probe makes it a promising tool for the unbiased analysis of glycosidase activities in diagnostic and drug-screening assays. This research also paves the way for the design of sensitive fluorescent probes for the detection of other enzymatic activities based on mixed photophysical mechanisms.<sup>37–41</sup>

## Conflicts of interest

The authors have no conflicts of interest to declare.

## Acknowledgements

The authors thank the Natural National Science Foundation of China (no. 91853201, 92253306 and 82151219), the Shanghai Municipal Science and Technology Major Project (no. 2018SHZDZX03), the Fundamental Research Funds for the Central Universities (222201717003), the Programme of Introducing Talents of Discipline to Universities (B16017) and the Open Funding Project of the State Key Laboratory of Bioreactor Engineering. TDJ wishes to thank the Open Research Fund of the School of Chemistry and Chemical Engineering, Henan Normal University for support (2020ZD01). The Research Center of Analysis and Test of East China University of Science and Technology is gratefully acknowledged for assistance in analytical experiments.

## Notes and references

- C. Reily, T. J. Stewart, M. B. Renfrow and J. Novak, Glycosylation in health and disease, *Nat. Rev. Nephrol.*, 2019, **15**, 346.



- 2 M. R. Pratt and C. R. Bertozzi, Synthetic glycopeptides and glycoproteins as tools for biology, *Chem. Soc. Rev.*, 2005, **34**, 58.
- 3 B. A. H. Smith and C. R. Bertozzi, The clinical impact of glycobiology: targeting selectins, Siglecs and mammalian glycans, *Nat. Rev. Drug Discovery*, 2021, **20**, 217.
- 4 B. Winchester, Lysosomal metabolism of glycoproteins, *Glycobiology*, 2005, **15**, 1R.
- 5 K. Ohtsubo and J. D. Marth, Glycosylation in Cellular Mechanisms of Health and Disease, *Cell*, 2006, **126**, 855.
- 6 B. Y. Lee, J. A. Han, J. S. Im, A. Morrone, K. Johung, E. C. Goodwin, W. J. Kleijer, D. DiMaio and E. S. Hwang, Senescence-associated  $\beta$ -galactosidase is lysosomal  $\beta$ -galactosidase, *Aging Cell*, 2006, **5**, 187.
- 7 D. G. Hildebrand, S. Lehle, A. Borst, S. Haferkamp, F. Essmann and K. Schulze-Osthoff,  $\alpha$ -Fucosidase as a novel convenient biomarker for cellular senescence, *Cell Cycle*, 2013, **12**, 1922.
- 8 S. K. Chatterjee, M. Bhattacharya and J. J. Barlow, Glycosyltransferase and glycosidase activities in ovarian cancer patients, *Cancer Res.*, 1979, **39**, 1943.
- 9 Y. Jiang, A. Sun, Y. Zhao, W. Ying, H. Sun, X. Yang, B. Xing, W. Sun, L. Ren, B. Hu, C. Li, L. Zhang, G. Qin, M. Zhang, N. Chen, M. Zhang, Y. Huang, J. Zhou, Y. Zhao, M. Liu, X. Zhu, Y. Qiu, Y. Sun, C. Huang, M. Yan, M. Wang, W. Liu, F. Tian, H. Xu, J. Zhou, Z. Wu, T. Shi, W. Zhu, J. Qin, L. Xie, J. Fan, X. Qian, F. He and Chinese Human Proteome Project (CNHPP) Consortium, Proteomics identifies new therapeutic targets of early-stage hepatocellular carcinoma, *Nature*, 2019, **567**, 257.
- 10 J.-J. Zhang, X.-Z. Chai, X.-P. He, H.-J. Kim, J. Y. Yoon and H. Tian, Fluorogenic probes for disease-relevant enzymes, *Chem. Soc. Rev.*, 2019, **48**, 683.
- 11 X.-L. Hu, H.-Q. Gan, F.-D. Meng, H.-H. Han, D.-T. Shi, S. Zhang, L. Zou, X.-P. He and T. D. James, Fluorescent probes and functional materials for biomedical applications, *Front. Chem. Sci. Eng.*, 2022, **16**, 1425.
- 12 W.-T. Dou, H.-H. Han, A. C. Sedgwick, G.-B. Zhu, Y. Zang, X.-R. Yang, J. Y. Yoon, T. D. James, J. Li and X.-P. He, Fluorescent probes for the detection of disease-associated biomarkers, *Sci. Bull.*, 2022, **67**, 853.
- 13 H. Singh, K. Tiwari, R. Tiwari, S. K. Pramanik and A. Das, Small Molecule as Fluorescent Probes for Monitoring Intracellular Enzymatic Transformations, *Chem. Rev.*, 2019, **119**, 11718.
- 14 X.-H. Li, X.-H. Gao, W. Shi and H.-M. Ma, Design Strategies for Water-Soluble Small Molecular Chromogenic and Fluorogenic Probes, *Chem. Rev.*, 2014, **114**, 590.
- 15 H.-W. Liu, L.-L. Chen, C.-Y. Xu, Z. Li, H.-Y. Zhang, X.-B. Zhang and W.-H. Tan, Recent progresses in small-molecule enzymatic fluorescent probes for cancer imaging, *Chem. Soc. Rev.*, 2018, **47**, 7140.
- 16 X.-F. Wu, R. Wang, N. Kwon, M.-H. Ma and J.-Y. Yoon, Activatable fluorescent probes for in situ imaging of enzymes, *Chem. Soc. Rev.*, 2022, **51**, 450.
- 17 H.-D. Li, D. Kim, Q.-C. Yao, H.-Y. Ge, J. Chung, J.-L. Fan, J.-Y. Wang, X.-J. Peng and J.-Y. Yoon, Activity-Based NIR Enzyme Fluorescent Probes for the Diagnosis of Tumors and Image-Guided Surgery, *Angew. Chem., Int. Ed.*, 2021, **60**, 17268.
- 18 Y. Urano, M. Kamiya, K. Kanda, T. Ueno, K. Hirose and T. Nagano, Evolution of Fluorescein as a Platform for Finely Tunable Fluorescence Probes, *J. Am. Chem. Soc.*, 2005, **127**, 4888.
- 19 G.-Y. Jiang, G.-J. Zeng, W.-P. Zhu, Y.-D. Li, X.-B. Dong, G.-X. Zhang, X.-L. Fan, J.-G. Wang, Y.-Q. Wu and B.-Z. Tang, A selective and light-up fluorescent probe for  $\beta$ -galactosidase activity detection and imaging in living cells based on an AIE tetraphenylethylene derivative, *Chem. Commun.*, 2017, **53**, 4505.
- 20 K.-Z. Gu, Y.-S. Xu, H. Li, Z.-Q. Guo, S.-J. Zhu, S.-Q. Zhu, P. Shi, T. D. James, H. Tian and W.-H. Zhu, Real-Time Tracking and In Vivo Visualization of  $\beta$ -Galactosidase Activity in Colorectal Tumor with a Ratiometric Near-Infrared Fluorescent Probe, *J. Am. Chem. Soc.*, 2016, **138**, 5334.
- 21 X.-K. Li, W.-J. Qiu, J.-W. Li, X. Chen, Y.-L. Hu, Y. Gao, D.-L. Shi, X.-M. Li, H.-L. Lin, Z.-L. Hu, G.-Q. Dong, C.-Q. Sheng, B. Jiang, C.-L. Xia, C.-Y. Kim, Y. Guo and J. Li, First-generation species-selective chemical probes for fluorescence imaging of human senescence-associated  $\beta$ -galactosidase, *Chem. Sci.*, 2020, **11**, 7292.
- 22 K.-Z. Gu, W.-S. Qiu, Z.-Q. Guo, C.-X. Yan, S.-Q. Zhu, D.-F. Yao, P. Shi, H. Tian and W.-H. Zhu, An enzyme-activatable probe liberating AIEgens: on-site sensing and long-term tracking of  $\beta$ -galactosidase in ovarian cancer cells, *Chem. Sci.*, 2019, **10**, 398.
- 23 D. Asanuma, M. Sakabe, M. Kamiya, K. Yamamoto, J. Hiratake, M. Ogawa, N. Kosaka, P. L. Choyke, T. Nagano, H. Kobayashi and Y. Urano, Sensitive  $\beta$ -galactosidase-targeting fluorescence probe for visualizing small peritoneal metastatic tumours in vivo, *Nat. Commun.*, 2015, **6**, 6463.
- 24 S. Cecioni, R. A. Ashmus, P.-A. Gilormini, S. Zhu, X. Chen, X.-Y. Shan, C. Gros, M. C. Deen, Y. Wang, R. Britton and D. J. Vocadlo, Quantifying lysosomal glycosidase activity within cells using bis-acetal substrates, *Nat. Chem. Biol.*, 2022, **18**, 332.
- 25 A. K. Yadav, D. L. Shen, X.-Y. Shan, X. He, A. R. Kermode and D. J. Vocadlo, Fluorescence-Quenched Substrates for Live Cell Imaging of Human Glucocerebrosidase Activity, *J. Am. Chem. Soc.*, 2015, **137**, 1181.
- 26 S.-J. Chen, X.-D. Ma, L. Wang, Y.-Y. Wu, Y.-P. Wang, W.-K. Fan and S.-C. Hou, Design and application of lysosomal targeting pH-sensitive  $\beta$ -galactosidase fluorescent probe, *Sens. Actuators, B*, 2023, **379**, 133272.
- 27 L. Dong, M.-Y. Zhang, H.-H. Han, Y. Zang, G.-R. Chen, J. Li, X.-P. He and S. Vidal, A General Strategy to the Intracellular Sensing of Glycosidases using AIE-Based Glycoclusters, *Chem. Sci.*, 2022, **13**, 247.
- 28 Z.-G. Song, R. T. K. Kwok, E.-G. Zhao, Z.-K. He, Y.-N. Hong, J. W. Y. Lam, B. Liu and B.-Z. Tang, A Ratiometric



- Fluorescent Probe Based on ESIPT and AIE Processes for Alkaline Phosphatase Activity Assay and Visualization in Living Cells, *ACS Appl. Mater. Interfaces*, 2014, **6**, 17245.
- 29 Y. Liu, J. Nie, J. Niu, W.-S. Wang and W.-Y. Lin, An AIE + ESIPT ratiometric fluorescent probe for monitoring sulfur dioxide with distinct ratiometric fluorescence signals in mammalian cells, mouse embryonic fibroblast and zebrafish, *J. Mater. Chem. B*, 2018, **6**, 1973.
- 30 G.-L. Zeng, Z.-H. Liang, X. Jiang, T.-T. Quan and T.-S. Chen, An ESIPT-Dependent AIE Fluorophore Based on HBT Derivative: Substituent Positional Impact on Aggregated Luminescence and its Application for Hydrogen Peroxide Detection, *Chem. – Eur. J.*, 2022, **28**, e202103241.
- 31 Q. Chen, C.-M. Jia, Y.-F. Zhang, W. Du, Y. Wang, Y. Huang, Q.-Y. Yanga and Q. Zhang, A novel fluorophore based on the coupling of AIE and ESIPT mechanisms and its application in biothiol imaging, *J. Mater. Chem. B*, 2017, **5**, 7736.
- 32 A. C. Sedgwick, L.-L. Wu, H.-H. Han, S. D. Bull, X.-P. He, T. D. James, J. L. Sessler, B.-Z. Tang, H. Tian and J. Yoon, Excited-state intramolecular proton-transfer (ESIPT) based fluorescence sensors and imaging agents, *Chem. Soc. Rev.*, 2018, **47**, 8842.
- 33 C. Rivasa, M. Kamiya and Y. Urano, A novel sialidase-activatable fluorescence probe with improved stability for the sensitive detection of sialidase, *Bioorg. Med. Chem.*, 2020, **30**, 126860.
- 34 X. Feng, C.-X. Qi, H.-T. Feng, Z. Zhao, H. H. Y. Sung, L. D. Williams, R. T. K. Kwok, J. W. Y. Lam, A. Qin and B.-Z. Tang, Dual fluorescence of tetraphenylethylene-substituted pyrenes with aggregation-induced emission characteristics for white-light emission, *Chem. Sci.*, 2018, **9**, 5679.
- 35 N. A. Kukhta and M. R. Bryce, Dual emission in purely organic materials for optoelectronic applications, *Mater. Horiz.*, 2021, **8**, 33.
- 36 S. K. Behera, S. Y. Park and J. Gierschner, Dual Emission: Classes, Mechanisms, and Conditions, *Angew. Chem., Int. Ed.*, 2021, **60**, 22624.
- 37 W.-T. Dou, X. Wang, T. Liu, S.-W. Zhao, J.-J. Liu, Y. Yan, J. Li, C.-Y. Zhang, A. C. Sedgwick, H. Tian, J. L. Sessler, D.-M. Zhou and X.-P. He, A homogeneous high-throughput array for the detection and discrimination of influenza A viruses, *Chem*, 2022, **8**, 1750.
- 38 W.-T. Dou, Z.-Y. Qin, J. Li, D.-M. Zhou and X.-P. He, Self-assembled sialyllactosyl probes with aggregation-enhanced properties for ratiometric detection and blocking of influenza viruses, *Sci. Bull.*, 2019, **64**, 1902.
- 39 W.-T. Dou, W. Chen, X.-P. He, J. Su and H. Tian, Vibration-Induced-Emission (VIE) for imaging amyloid  $\beta$  fibrils, *Faraday Discuss.*, 2017, **196**, 395.
- 40 A. C. Sedgwick, K.-C. Yan, D. N. Mangel, Y. Shang, A. Steinbrueck, H.-H. Han, J. T. Brewster, X.-L. Hu, D. W. Snelson, V. M. Lynch, H. Tian, X.-P. He and J. L. Sessler, Deferasirox (ExJade): An FDA-Approved AIEgen Platform with Unique Photophysical Properties, *J. Am. Chem. Soc.*, 2020, **142**, 1925.
- 41 X.-L. Hu, A. C. Sedgwick, D. N. Mangel, Y. Shang, A. Steinbrueck, K.-C. Yan, L. Zhu, D. W. Snelson, S. Sen, C. V. Chau, G. Juarez, V. M. Lynch, X.-P. He and J. L. Sessler, Tuning the Solid- and Solution-State Fluorescence of the Iron Chelator Deferasirox, *J. Am. Chem. Soc.*, 2022, **144**, 7382.

